

Mixed-Integer Programming for Signal Temporal Logic with Fewer Binary Variables

Vince Kurtz and Hai Lin

Abstract—Signal Temporal Logic (STL) provides a convenient way of encoding complex control objectives for robotic and cyber-physical systems. The state-of-the-art in trajectory synthesis for STL is based on Mixed-Integer Convex Programming (MICP). The MICP approach is sound and complete, but has limited scalability due to exponential complexity in the number of binary variables. In this letter, we propose a more efficient MICP encoding for STL. Our new encoding is based on the insight that disjunction can be encoded using a logarithmic number of binary variables and conjunction can be encoded without binary variables. We demonstrate in simulation examples that our proposed approach significantly outperforms the state-of-the-art for long and complex specifications. Open-source software is available: <https://stlpy.readthedocs.io>.

Index Terms—Autonomous systems, Robotics, Optimization.

I. INTRODUCTION

SIGNAL Temporal Logic (STL) is a powerful means of expressing complex control objectives. STL combines boolean operators (“and”, “or”, “not”) with temporal operators (“always”, “eventually”, “until”) and is defined over continuous-valued signals, making it an appealing choice for dynamical systems ranging from mobile robots [1]–[3] and quadrotors [4] to high-DoF manipulators [5] and traffic networks [6], [7].

In this letter, we address the trajectory synthesis problem for discrete-time linear systems subject to STL specifications over convex predicates. That is, given a system and a specification, find a satisfying trajectory that minimizes a given cost.

The state-of-the-art solution uses Mixed-Integer Convex Programming (MICP) [8]. This approach, first proposed in [9] and later refined in [10], [11], is sound and complete: any solution returned by the algorithm satisfies the specification, and the algorithm finds a solution whenever one exists. Furthermore, MICP finds globally optimal solutions, enabling maximally robust or minimum energy trajectories.

The major limitation is scalability. MICP’s worst-case complexity is exponential in the number of binary variables, and the state-of-the-art in STL synthesis introduces a binary variable for each predicate at each timestep. This limits MICP methods to simple specifications and short time horizons [8].

This exponential complexity should not be too surprising. STL synthesis is NP-hard, so exponential worst-case complexity is inevitable for any sound and complete algorithm

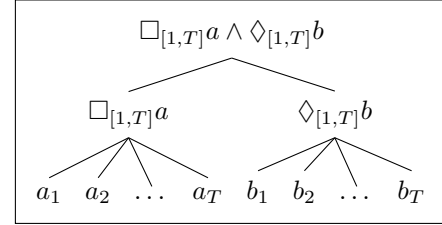


Fig. 1. Tree representation of the STL formula $\square_{[1,T]}a \wedge \diamond_{[1,T]}b$. For this example, our approach reduces the number of binary variables from $2T$ to $\lceil \log_2(T+1) \rceil$, reducing computational complexity from $O(2^{2T})$ to $O(T)$.

(assuming $P \neq NP$). But despite this NP-hardness, MICP performs well in practice for moderately sized problems. With this in mind, much research in STL synthesis has gone toward reducing MICP problem sizes. For example, rewriting formulas in Positive Normal Form (PNF) significantly reduces the number of binary variables and constraints [8], [11]. Waypoint-based abstractions can further limit the problem size [12].

Another possibility is to formulate MICPs with tighter convex relaxations. While this does not improve the worst-case complexity, a tighter convex relaxation increases branch-and-bound efficiency and often improves performance in practice [13]. This approach has been pursued for Metric Temporal Logic in [14] and piecewise-affine reachability in [15].

Much STL research in recent years has focused on avoiding MICP entirely, and instead designing efficient heuristic methods which are sound but not complete. Such methods include gradient-based optimization [2], [3], [16], [17], differential dynamic programming [5], control barrier functions [18] and neural-network-based methods [19]. These approaches tend to improve scalability, especially with respect to the specification time horizon, but offer limited formal guarantees and often struggle to handle more complex specifications.

In this letter, we return to STL synthesis via MICP and propose a new MICP encoding that uses fewer binary variables. Our proposed approach draws on a logarithmic encoding of SOS1 constraints [20] to reduce the number of binary variables. Similar to [8], [11], we consider formulas in PNF, but rather than introducing a binary variable for each predicate at each timestep, our proposed approach introduces binary variables only for disjunctive subformulas. Furthermore, each disjunctive subformula is encoded using a logarithmic number of binary variables. This approach leads to particularly notable reductions in complexity for long-horizon specifications, though the standard MICP encoding [8] tends to outperform our proposed approach for short horizons.

For example, consider the specification shown in Figure 1,

The authors are with the Departments of Electrical Engineering, University of Notre Dame, Notre Dame, IN, 46556 USA. {vkurtz, hlin1}@nd.edu
This work was supported by NSF Grants CNS-1830335, IIS-2007949.

which reads “always a and eventually b ”. The standard MICP encoding requires a linear number of binary variables with respect to time horizon T , resulting in exponential computational complexity. Our proposed encoding uses a logarithmic number of binary variables, resulting in linear complexity.

Our primary contributions are as follows:

- We propose a new MICP encoding for STL specifications that uses fewer binary variables for most specifications,
- Our proposed approach is sound and complete, and guaranteed to find a globally optimal solution,
- We propose a tree data structure for STL formulas, and show how this data structure can be exploited to further reduce the number of binary variables,
- We demonstrate the scalability of our approach in various simulated scenarios involving a mobile robot. Code for reproducing these results is available online [21].

The remainder of this letter is organized as follows: background and a formal problem statement are presented in Section II, our main results are presented in Section III, and simulation experiments are reported in Section IV.

II. BACKGROUND

A. System Definitions

In this letter, we consider discrete-time linear systems:

$$\begin{aligned} \mathbf{x}_{t+1} &= \mathbf{A}\mathbf{x}_t + \mathbf{B}\mathbf{u}_t, \\ \mathbf{y}_t &= \mathbf{C}\mathbf{x}_t + \mathbf{D}\mathbf{u}_t, \end{aligned} \quad (1)$$

where $\mathbf{x}_t \in X \subseteq \mathbb{R}^n$ is the system state at timestep t , $\mathbf{u}_t \in U \subseteq \mathbb{R}^m$ is the control input, and $\mathbf{y}_t \in Y \subseteq \mathbb{R}^p$ is the output. We assume that X , U and Y are convex sets, and \mathbf{A} , \mathbf{B} , \mathbf{C} , \mathbf{D} are matrices of appropriate dimension.

Given an initial state \mathbf{x}_0 and a control tape $\mathbf{u} = \mathbf{u}_0, \mathbf{u}_1, \dots$, the output signal $\mathbf{y} = \mathbf{y}_0, \mathbf{y}_1, \dots$ is generated by applying (1). We denote the output signal starting at timestep t by

$$(\mathbf{y}, t) = \mathbf{y}_t, \mathbf{y}_{t+1}, \mathbf{y}_{t+2}, \dots$$

B. Signal Temporal Logic

We consider STL formulas over convex predicates in PNF: further details and discussion of STL formulas can be found in [8]. Such formulas follow the syntax

$$\varphi := \pi \mid \bigvee_i \varphi_i \mid \bigwedge_i \varphi_i \mid \square_{[t_1, t_2]} \varphi \mid \diamond_{[t_1, t_2]} \varphi \mid \varphi_1 \mathcal{U}_{[t_1, t_2]} \varphi_2, \quad (2)$$

where predicates π are defined by convex functions $g^\pi : Y \rightarrow \mathbb{R}$ such that $\{\mathbf{y} \mid g^\pi(\mathbf{y}) \leq 0\}$ are convex sets. In addition to standard boolean operations “and” (\wedge) and “or” (\vee), STL includes temporal operators “always” (\square), “eventually” (\diamond) and “until” (\mathcal{U}). In this letter we consider only bounded-time specifications, i.e., those with t_2 finite.

Remark 1. *This syntax is slightly more general than that with linear predicates only, as considered in [9]–[12], since such convex predicates include linear ones $g^\pi(\mathbf{y}_t) = \mathbf{a}^T \mathbf{y}_t - b$. Note*

that negation (\neg) can be applied to linear predicates, but not to more general convex predicates such as ellipses.

The semantics, or meaning, of STL formulas are defined as follows, where we denote the fact that signal \mathbf{y} satisfies specification φ as $\mathbf{y} \models \varphi$. Here we present the quantitative semantics of STL, which defines a scalar “robustness value” $\rho^\varphi(\mathbf{y})$ which is positive only if $\mathbf{y} \models \varphi$:

- $\mathbf{y} \models \varphi$ if and only if $\rho^\varphi((\mathbf{y}, 0)) \geq 0$
- $\rho^\pi((\mathbf{y}, t)) = -g^\pi(\mathbf{y}_t)$, since $\mathbf{y} \models \pi$ if $g^\pi(\mathbf{y}_0) \leq 0$
- $\rho^{\varphi_1 \wedge \varphi_2}((\mathbf{y}, t)) = \min(\rho^{\varphi_1}((\mathbf{y}, t)), \rho^{\varphi_2}((\mathbf{y}, t)))$
- $\rho^{\varphi_1 \vee \varphi_2}((\mathbf{y}, t)) = \max(\rho^{\varphi_1}((\mathbf{y}, t)), \rho^{\varphi_2}((\mathbf{y}, t)))$
- $\rho^{\diamond_{[t_1, t_2]} \varphi}((\mathbf{y}, t)) = \max_{t' \in [t+t_1, t+t_2]} (\rho^\varphi((\mathbf{y}, t')))$
- $\rho^{\square_{[t_1, t_2]} \varphi}((\mathbf{y}, t)) = \min_{t' \in [t+t_1, t+t_2]} (\rho^\varphi((\mathbf{y}, t')))$
- $\rho^{\varphi_1 \mathcal{U}_{[t_1, t_2]} \varphi_2}((\mathbf{y}, t)) = \max_{t' \in [t+t_1, t+t_2]} \left(\min \left(\left[\rho^{\varphi_1}((\mathbf{y}, t')), \min_{t'' \in [t+t_1, t'] } (\rho^{\varphi_2}((\mathbf{y}, t''))) \right] \right) \right)$.

For a given STL formula φ , we denote the time horizon (minimum number of timesteps after which a signal’s satisfaction status is fixed) as T . We denote the number of predicates as N^π and the number of disjunctive subformulas as N^\vee :

Definition 1. *Disjunctive (sub)formulas are defined as follows:*

- π , $\bigwedge_{j=1}^n \varphi_j$, and $\diamond_{[t_1, t_2]} \varphi_i$ are not disjunctive;
- $\bigvee_{j=1}^k \varphi_i$ is disjunctive, with k disjunctions;
- $\diamond_{[t_1, t_2]} \varphi$ is disjunctive, with $t_2 - t_1$ disjunctions;
- $\varphi_1 \mathcal{U}_{[t_1, t_2]} \varphi_2$ is disjunctive, with $t_2 - t_1$ disjunctions.

We denote the number of disjunctions associated with the i^{th} disjunctive subformula as N_i . For example, the formula $(a \vee b) \wedge \diamond_{[0, T]} c$ has two disjunctive subformulas, with $N_1 = 2$ and $N_2 = T + 1$ respectively.

C. Problem Statement

Given an initial state, an STL specification, and a quadratic running cost, our problem is to find a minimum cost trajectory that satisfies the STL specification. More formally, this problem can be stated as an optimization problem:

Problem 1. *Given a system of the form (1), an initial state \mathbf{x}_0 , and an STL specification φ , solve the optimization problem*

$$\min_{\mathbf{x}, \mathbf{u}, \mathbf{y}} -\rho^\varphi(\mathbf{y}) + \sum_{t=0}^T \mathbf{x}_t^T \mathbf{Q} \mathbf{x}_t + \mathbf{u}_t^T \mathbf{R} \mathbf{u}_t \quad (3a)$$

$$\text{s.t. } \mathbf{x}_{t+1} = \mathbf{A}\mathbf{x}_t + \mathbf{B}\mathbf{u}_t \quad (3b)$$

$$\mathbf{y}_t = \mathbf{C}\mathbf{x}_t + \mathbf{D}\mathbf{u}_t \quad (3c)$$

$$\mathbf{x}_0 \text{ fixed} \quad (3d)$$

$$\mathbf{x}_t \in X, \mathbf{u}_t \in U, \mathbf{y}_t \in Y \quad (3e)$$

$$\rho^\varphi(\mathbf{y}) \geq 0 \quad (3f)$$

where $\mathbf{Q} \succeq 0$ and $\mathbf{R} \succeq 0$ are symmetric cost matrices.

Apart from the robustness measure $\rho^\varphi(\mathbf{y})$, (3) is a convex optimization problem, for which many mature solvers exist

[22]. With this in mind, our primary goal is to introduce mixed-integer constraints to define $\rho^\varphi(\mathbf{y})$, preferably using as few binary variables as possible.

Remark 2. Note that with $\mathbf{Q} = \mathbf{R} = 0$, this optimization problem maximizes the robustness measure ρ , resulting in a maximally satisfying solution. Similarly, the cost matrices \mathbf{Q} and \mathbf{R} can be scaled to trade off maximizing STL satisfaction and minimizing the running cost.

III. MAIN RESULTS

The current state-of-the-art is to encode (3) as an MICP with TN^π binary variables (one per predicate per timestep) [8]. In this section, we propose an encoding with $\sum_{i=1}^{N^\vee} \lceil \log_2(N_i + 1) \rceil$ binary variables, where N_i is the number of disjunctions associated with the i^{th} disjunctive subformula. Note that N_i may vary with the time horizon T , depending on the specification.

We first introduce a tree data structure for representing STL formulas. Then, after presenting our proposed encoding, we show how simple offline operations on this data structure can further reduce the number of binary variables.

A. Representing STL Specifications

In this section, we present a tree data structure for STL formulas. A similar approach was taken in [17], with the primary aim of enabling efficient gradient-based optimization. Here, our primary aim is to enable more efficient MICP.

Our tree data structure is formally defined as follows:

Definition 2. An STL Tree \mathcal{T}^φ is a tuple $(S, \tau, \circ, \rho^\varphi)$, where

- $S = [\mathcal{T}^{\varphi_1}, \mathcal{T}^{\varphi_2}, \dots, \mathcal{T}^{\varphi_N}]$ is a list of N subtrees (i.e., children) associated with each subformula;
- $\tau = [t^{\varphi_1}, t^{\varphi_2}, \dots, t^{\varphi_N}]$ is a list of time steps corresponding to the N subformulas;
- $\circ \in \{\wedge, \vee\}$ is a combination type;
- ρ^φ is the STL robustness measure: a function which maps signals \mathbf{y} to scalar values.

All nodes in an STL Tree are themselves STL Trees, and correspond to subformulas. Leaves of an STL Tree correspond to predicates π . For a given STL formula φ , a corresponding tree \mathcal{T}^φ can be built up recursively by following the syntax presented in Section II-B.

Example 1. Consider the specification $\varphi = \square_{[1,T]} a \wedge \diamond_{[1,T]} b$, where a and b are predicates. The associated STL Tree is shown in Figure 1. There are two \wedge -type nodes (associated with φ and $\square a$), one \vee -type node ($\diamond b$), and $2T$ predicates.

Roughly speaking, the original MICP encoding of [9] introduces a binary variable for each node in this tree, while [11] introduces a binary variable for each leaf¹. Our proposed encoding, outlined in the following section, instead introduces binary variables only for disjunctive nodes. Furthermore, each disjunctive node only introduces $\lceil \log_2(N + 1) \rceil$ binary variables, where N is the number of subformulas.

¹More precisely, [11] introduces a binary variable for each predicate at each timestep. This is typically slightly more than the number of leaves.

B. New Mixed-Integer Encoding

We now present our proposed mixed-integer encoding. Given an STL formula φ , we start by constructing a corresponding STL Tree \mathcal{T}^φ . We define a continuous variable $\rho \geq 0$ which, with some liberty of notation, will provide a lower bound on the robustness measure $\rho^\varphi(\mathbf{y})$. Note that if the robustness measure is negative, a violation of the constraint $\rho \geq 0$ will render the optimization problem infeasible.

For each node \mathcal{T}^ϕ in the tree, we introduce a *continuous* variable $z^\phi \in [0, 1]$. Ultimately, we will add constraints such that $z^\phi = 1$ if subformula ϕ is enforced and $z^\phi = 0$ otherwise. While these variables take binary values, declaring them as continuous improves MICP efficiency, since MICP complexity is dominated by the number of binary variables.

We start with the leaf nodes. Each leaf is associated with a predicate (π) and a timestep t . For each leaf we constrain

$$\rho \leq -g^\pi(\mathbf{y}_t) + M(1 - z^\pi), \quad (4)$$

where M is a large scalar constant. This “big-M” constraint enforces $\rho \leq -g^\pi(\mathbf{y}_t)$ if $z^\pi = 1$, but leaves ρ and \mathbf{y}_t essentially unconstrained if $z^\pi = 0$ [13].

Next we consider all of the \wedge -type nodes in the tree. For the corresponding formula ϕ to hold, all of the subformulas $\phi_1, \phi_2, \dots, \phi_N$ must also hold. In other words, $z^\phi = 1$ implies $z^{\phi_i} = 1$. This can be encoded without adding binary variables, simply by applying the linear constraints:

$$z^\phi \leq z^{\phi_i} \quad \forall i = 1, 2, \dots, N. \quad (5)$$

Disjunctive constraints present more of a challenge. For these \vee -type constraints, we need to enforce at least one $z^{\phi_i} = 1$ if $z^\phi = 1$. A natural way to do this would be to define z^{ϕ_i} as binary variables and add the constraint:

$$z^\phi \leq \sum_{i=1}^N z^{\phi_i}.$$

This approach was taken in [9], and adds N binary variables.

We now show how results in disjunctive programming [20] can be leveraged to encode disjunctive constraints using only $\log_2(N + 1)$ binary variables. To introduce these constraints, we first define SOS1 sets:

Definition 3. A vector $\lambda = [\lambda_1, \lambda_2, \dots, \lambda_n]^T$ is a *Special Ordered Set of Type 1 (SOS1)* if the following conditions hold:

- $\lambda_i \geq 0$
- $\sum_i \lambda_i = 1$
- $\exists j \in [1, \dots, n]$ s.t. $\lambda_j = 1$

In other words, a vector λ is in SOS1 if it contains exactly one nonzero element, and that element is equal to 1.

Perhaps surprisingly, we can constrain $\lambda \in \text{SOS1}$ using a logarithmic number of binary variables and constraints:

Theorem 1 ([20]). Assume that n is a power of 2. Let $I = 1, 2, \dots, n$ and $B : I \rightarrow \{0, 1\}^{\log_2(n)}$ be any bijective function. Then the following constraints enforce $\lambda \in \text{SOS1}$:

$$\begin{aligned} \lambda_i &\geq 0, \quad \sum_i \lambda_i = 1, \\ \sum_{j \in J^+(k, B)} \lambda_j &\leq \zeta_k, \quad \sum_{j \in J^0(k, B)} \lambda_j \leq (1 - \zeta_k) \\ \zeta_k &\in \{0, 1\} \quad \forall k \in [1, 2, \dots, \log_2(n)] \end{aligned}$$

where $J^+(k, B) = \{i \mid k \in \text{supp}(B(i))\}$, $J^0(k, B) = \{i \mid k \notin \text{supp}(B(i))\}$, and $\text{supp}(B(i))$ denotes the support of $B(i)$.

For the bijective function $B(i)$, the mapping from index i to its binary representation is a natural choice. In that case, the values of binary variables ζ_k essentially represent which index i is holds the nonzero value. If n is not a power of 2, we can simply add $e^{\lceil \log_2 n \rceil} - n$ elements along with linear constraints $\lambda_i = 0$ that force these elements to be zero.

This brings us back to encoding disjunctive STL subformulas. For these \vee -type nodes in the STL tree, we need $z^\phi \implies \bigvee_{i=1}^N z^{\phi_i}$. This can be written as a SOS1 constraint

$$[1 - z^\phi, z^{\phi_1}, z^{\phi_2}, \dots, z^{\phi_N}] \in \text{SOS1}, \quad (6)$$

which can be encoded with $\lceil \log_2(N + 1) \rceil$ binary variables.

Note that SOS1 ensures *exactly* one nonzero element, while disjunction requires *at least* one nonzero element. This is not an issue, however, because we only need a sufficient (not necessary) condition for $\mathbf{y} \models \phi$. Focusing on specifications in PNF allows us to guarantee both soundness and completeness while only requiring this sort of sufficient condition [8], [11].

Finally, for the root node we constrain

$$z^\varphi = 1, \quad (7)$$

to ensure that the overall specification φ must be satisfied.

Proposition 1. If the constraints (4)-(7) are met, then the following properties hold:

- 1) The continuous variable z^ϕ is 1 only if $\mathbf{y} \models \phi$;
- 2) The decision variable ρ provides a lower bound for the robustness measure $\rho^\varphi(\mathbf{y})$;
- 3) The constraints (4)-(7) are feasible if and only if $\mathbf{y} \models \varphi$.

Proof. Property 1 follows naturally from Theorem 1 and the reasoning of [9]. Note that this property is one-directional: it may be the case that $z^\phi = 0$ and $\mathbf{y} \models \phi$ for some subformula.

Property 2 follows from the definition of the robustness measure and constraints (4).

For Property 3, the reverse direction (only if) follows directly from Property 1 and constraint (7). The forward direction (if) follows from Property 2 and the constraint $\rho \geq 0$. \square

This allows us to solve Problem 1 as an MICP:

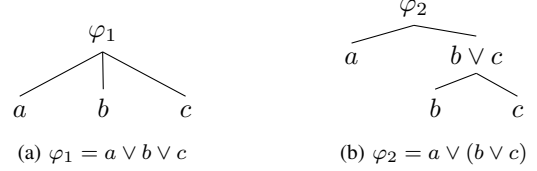


Fig. 2. STL Trees for two logically equivalent formulas. Our approach introduces 2 binary variables for φ_1 , but 4 variables for φ_2 .

$$\min_{\mathbf{x}, \mathbf{u}, \mathbf{y}, z^{\phi_i}, \rho} -\rho + \sum_{t=0}^T \mathbf{x}_t^T \mathbf{Q} \mathbf{x}_t + \mathbf{u}_t^T \mathbf{R} \mathbf{u}_t \quad (8a)$$

$$\text{s.t. Dynamics constraints (3b-3e)} \quad (8b)$$

$$\text{STL Constraints (4-7)} \quad (8c)$$

$$\rho \geq 0 \quad (8d)$$

Similar to the existing MICP encodings [8]–[11], this MICP is sound, complete, and globally optimal:

Theorem 2 (Sound and Complete). A dynamically feasible output signal \mathbf{y} is a solution to Problem 1 if and only if \mathbf{y} is a solution to (8).

Theorem 3 (Globally Optimal). If Problem 1 is feasible, the MICP (8) finds a globally optimal solution.

The advantage of our approach over other sound, complete, and globally optimal methods [8]–[11] is that our approach typically uses fewer binary variables. For many specifications, like that shown in Figure 1 and the examples in Section IV, this difference is quite significant.

It is possible, however, for our approach to have more binary variables than the standard encoding, particularly for specifications with few predicates but many nested disjunctions. To this end, the next section shows how the STL Tree data structure can be used to further reduce the MICP size.

C. Formula Flattening

Unlike the state-of-the-art MICP encoding with binary variables for every predicate at every timestep [8], the number of binary variables in our proposed encoding depends heavily on the structure of the STL Tree \mathcal{T}^φ . Since logically equivalent formulas can have different tree structures, this can have a major impact on solver efficiency.

For example, consider the logically equivalent formulas $\varphi_1 = a \vee b \vee c$ and $\varphi_2 = a \vee (b \vee c)$, where a , b , and c are predicates. STL Trees are illustrated in Figure 2. φ_1 includes one disjunctive subformula, and can be encoded with 2 binary variables. The logically equivalent φ_2 includes two disjunctive subformulas, however, and requires 4 binary variables.

Clearly, we should prefer “flatter” STL Trees for our proposed encoding. To this end, specification flattening provides an automatic means of compressing formulas with many layers into logically equivalent formulas with fewer layers. The basic idea is to search for nodes which have the same combination

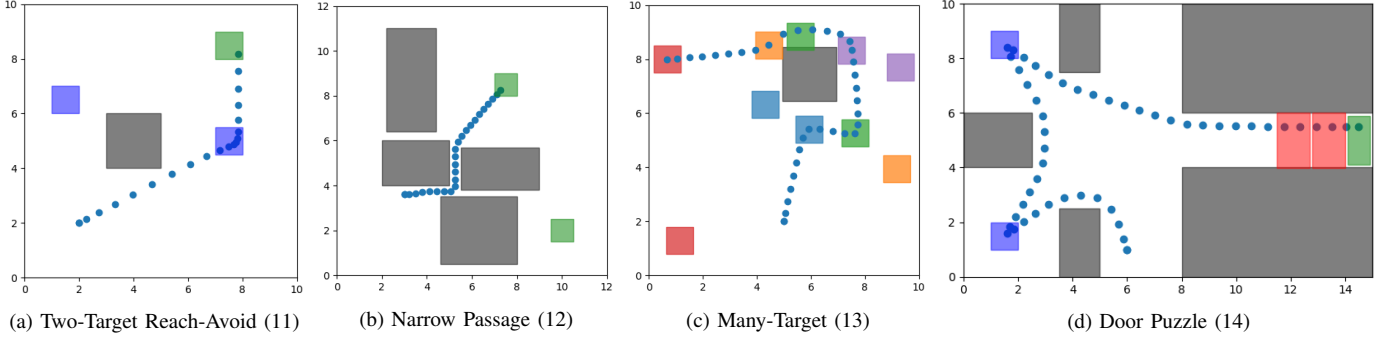


Fig. 3. Illustrations of example scenarios along with solutions generated by our proposed approach. Solve times are shown in Table I.

type (\wedge or \vee) as their parent. If this is the case, that node's children can be moved up a level and the node removed.

While formula flattening has the most dramatic impact on our proposed approach, it can also benefit other MICP encodings [8], [9], since flatter formulas introduce fewer continuous variables and constraints. Interestingly, while formula flattening consistently reduces the number of binary variables, it does not always improve solve times. We attribute this counter-intuitive result to the fact that certain solver-specific heuristics may be more effective on unflattened formulas. In Section IV, we only flatten formulas if it improves performance.

IV. SIMULATION EXPERIMENTS

In this section, we demonstrate the improved scalability of our proposed approach. This is largely due to a reduction in the number of binary variables — especially for specifications involving \diamond and \mathcal{U} over long time-horizons.

We consider several benchmark specifications involving a simple mobile robot exploring a planar environment. These specifications are illustrated in Figure 3. In all scenarios, we assume that the robot is governed by double-integrator dynamics in both the horizontal and vertical directions, i.e.,

$$\mathbf{x} = [p_x, p_y, \dot{p}_x, \dot{p}_y]^T \quad \mathbf{u} = [\ddot{p}_x, \ddot{p}_y]^T$$

where p_x is the horizontal position of the robot and p_y is the vertical position, in meters. The output signal is defined as $\mathbf{y} = [p_x, p_y]^T$, giving us dynamics

$$\mathbf{A} = \begin{bmatrix} \mathbf{I} & \mathbf{I} \\ \mathbf{0} & \mathbf{I} \end{bmatrix}, \quad \mathbf{B} = \begin{bmatrix} \mathbf{0} \\ \mathbf{I} \end{bmatrix}, \quad \mathbf{C} = [\mathbf{I} \quad \mathbf{0}], \quad \mathbf{D} = \mathbf{0}.$$

State and input constraints X and U are defined to enforce maximum acceleration and velocity of 0.5 m/s^2 and 1 m/s :

$$X = \{\mathbf{x} \mid 0 \leq p_x \leq 15, 0 \leq p_y \leq 15, |\dot{p}_x| \leq 1, |\dot{p}_y| \leq 1\}. \quad (9)$$

$$U = \{\mathbf{u} \mid |\ddot{p}_x| \leq 0.5, |\ddot{p}_y| \leq 0.5\}. \quad (10)$$

We used python and the Drake [23] mathematical programming interface to set up the MICP (8), and solved the MICP with Gurobi version 9.5.1 [24] with default options. As a baseline, we compare to the state-of-the-art MICP described in [8], similarly implemented in Drake/Gurobi. All experiments

were performed on a laptop with an Intel i7 processor and 32GB RAM. Open-source software is available online [21].

In the first scenario, shown in Figure 3a, our mobile robot must avoid an obstacle (O , grey), visit one of two intermediate targets (T_1, T_2 , blue) for at least 5 timesteps, and reach a goal (G , green). This specification can be written as

$$\diamond_{[0, T-5]}(\square_{[0, 5]}T_1 \vee \square_{[0, 5]}T_2) \wedge \square_{[0, T]} \neg O \wedge \diamond_{[0, T]}G, \quad (11)$$

where T is the specification time-bound.

The second scenario involves many obstacles and narrow passages, and is shown in Figure 3b. The robot must eventually reach one of two possible goals in addition to avoiding obstacles. This specification can be written as:

$$\diamond_{[0, T]}(G_1 \vee G_2) \wedge \square_{[0, T]} \left(\bigwedge_{i=1}^4 \neg O_i \right) \quad (12)$$

The third scenario, shown in Figure 3c, is designed to contain a more complex logical structure. In addition to avoiding an obstacle, the robot must visit several groups of targets T^j (red, green, blue, orange, and purple). There are two targets in each group, and at least one target from each group must be visited. This specification can be written as

$$\bigwedge_{i=1}^5 \left(\bigvee_{j=1}^2 \diamond_{[0, T]} T_i^j \right) \wedge \square_{[0, T]} (\neg O), \quad (13)$$

where T_i^j denotes the j^{th} target in group i .

The final scenario is inspired by [12], [25], and requires the robot to collect keys (i.e., visit blue regions) associated with certain doors (red) before reaching an end goal (green). This specification can be written as

$$\bigwedge_{i=1}^2 (\neg D_i \mathcal{U}_{[0, T]} K_i) \wedge \diamond_{[0, T]} G \wedge \square_{[0, T]} \left(\bigwedge_{i=1}^5 \neg O_i \right), \quad (14)$$

where K_i denotes picking up the i^{th} key and D_i denotes passing through the i^{th} door region.

Solve times and number of binary variables for each of these specifications over several time horizons T are shown in Table I. For all of these examples, our proposed approach uses fewer binary variables than the standard MICP [8]. The standard MICP is often faster for shorter time horizons, but our proposed encoding is consistently faster for long time horizons.

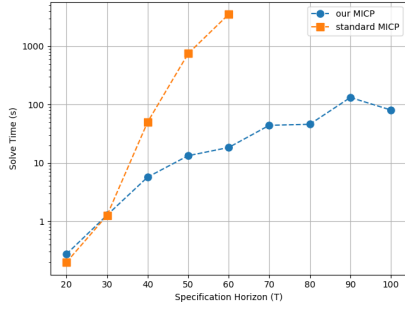


Fig. 4. Solve times for specification (11) over different time horizons.

Specification	Horizon (T)	Binary Vars.		Solve Time (s)	
		[8]	Ours	[8]	Ours
Two-Target (11)	25	1216	89	0.662	0.579
	50	2616	166	749	13.3
Narrow Passage (12)	25	624	318	2.27	5.92
	50	1124	619	168.8	158.1
Many-Target (13)	25	1144	441	3.36	16.8
	50	2244	846	>7500	2666
Door Puzzle (14)	25	3432	2355	8.46	8.75
	50	11832	8433	>7500	1392

TABLE I
SOLVE TIMES FOR BENCHMARK SCENARIOS

For specification (11), we provide a graph of solve times versus time horizon in Figure 4. Again, we see that our proposed approach outperforms the state-of-the-art for long time horizons, with the performance gap between the two approaches growing as T increases. This makes sense given how each approach introduces binary variables to handle the \diamond subformulas. Under the standard approach, the number of binary variables used to encode $\diamond_{[0,T]}$ increases linearly with T . Under our proposed approach, the number of binary variables increases only logarithmically.

Finally, we note that the standard MICP’s superior performance over short time horizons may be due to Gurobi’s presolve routines taking advantage of the extra binary variables to perform additional simplifications. Take, for example, the narrow passage specification (12) with 25 timesteps. With presolve enabled, the standard approach outperforms our approach (Table I). With presolve disabled, however, the standard approach takes over an hour to find an optimal solution, while our approach takes about a minute.

V. CONCLUSION

We proposed a more efficient mixed-integer encoding for Signal Temporal Logic. Our primary insight is that we can encode disjunctions using a logarithmic number of binary variables, and conjunctions without introducing any binary variables. We also introduced a tree data structure for STL, and showed how this data structure can be exploited to further reduce the number of binary variables and constraints. We demonstrated the improved scalability of our approach in simulation examples, where our proposed encoding outperformed the state-of-the-art by orders of magnitude on long and complex specifications.

REFERENCES

- [1] L. Lindemann, J. Nowak, L. Schönbacher, M. Guo, J. Tumova, and D. V. Dimarogonas, “Coupled multi-robot systems under linear temporal logic and signal temporal logic tasks,” *IEEE Transactions on Control Systems Technology*, vol. 29, no. 2, pp. 858–865, 2019.
- [2] Y. Gilpin, V. Kurtz, and H. Lin, “A smooth robustness measure of signal temporal logic for symbolic control,” *IEEE Control Systems Letters*, vol. 5, no. 1, pp. 241–246, 2021.
- [3] N. Mehdipour, C.-I. Vasile, and C. Belta, “Arithmetic-geometric mean robustness for control from signal temporal logic specifications,” in *2019 American Control Conference (ACC)*. IEEE, 2019, pp. 1690–1695.
- [4] Y. V. Pant, H. Abbas, R. A. Quaye, and R. Mangharam, “Fly-by-logic: control of multi-drone fleets with temporal logic objectives,” in *2018 ACM/IEEE 9th International Conference on Cyber-Physical Systems (ICCP)*. IEEE, 2018, pp. 186–197.
- [5] V. Kurtz and H. Lin, “Trajectory optimization for high-dimensional nonlinear systems under stl specifications,” *IEEE Control Systems Letters*, vol. 5, no. 4, pp. 1429–1434, 2020.
- [6] S. Sadraddini and C. Belta, “Model predictive control of urban traffic networks with temporal logic constraints,” in *2016 American Control Conference (ACC)*. IEEE, 2016, pp. 881–881.
- [7] S. Coogan, E. A. Gol, M. Arcak, and C. Belta, “Traffic network control from temporal logic specifications,” *IEEE Transactions on Control of Network Systems*, vol. 3, no. 2, pp. 162–172, 2015.
- [8] C. Belta and S. Sadraddini, “Formal methods for control synthesis: An optimization perspective,” *Annual Review of Control, Robotics, and Autonomous Systems*, vol. 2, pp. 115–140, 2019.
- [9] V. Raman, A. Donzé, M. Maasoumy, R. M. Murray, A. Sangiovanni-Vincentelli, and S. A. Seshia, “Model predictive control with signal temporal logic specifications,” in *53rd IEEE Conference on Decision and Control*. IEEE, 2014, pp. 81–87.
- [10] S. Sadraddini and C. Belta, “Robust temporal logic model predictive control,” in *2015 53rd Annual Allerton Conference on Communication, Control, and Computing (Allerton)*, sep 2015, pp. 772–779.
- [11] —, “Formal synthesis of control strategies for positive monotone systems,” *IEEE Transactions on Automatic Control*, vol. 64, no. 2, pp. 480–495, 2018.
- [12] D. Sun, J. Chen, S. Mitra, and C. Fan, “Multi-agent motion planning from signal temporal logic specifications,” *arXiv preprint arXiv:2201.05247*, 2022.
- [13] M. Conforti, G. Cornuéjols, G. Zambelli *et al.*, *Integer programming*. Springer, 2014, vol. 271.
- [14] V. Kurtz and H. Lin, “A more scalable mixed-integer encoding for metric temporal logic,” *IEEE Control Systems Letters*, 2021.
- [15] T. Marcucci, J. Umenberger, P. A. Parrilo, and R. Tedrake, “Shortest paths in graphs of convex sets,” *arXiv preprint arXiv:2101.11565*, 2021.
- [16] Y. V. Pant, H. Abbas, and R. Mangharam, “Smooth operator: Control using the smooth robustness of temporal logic,” in *Conference on Control Technology and Applications*. IEEE, 2017, pp. 1235–1240.
- [17] K. Leung, N. Aréchiga, and M. Pavone, “Back-propagation through signal temporal logic specifications: Infusing logical structure into gradient-based methods,” in *14th International Workshop on the Algorithmic Foundations of Robotics*, 2020.
- [18] L. Lindemann and D. V. Dimarogonas, “Control barrier functions for signal temporal logic tasks,” *IEEE Control Systems Letters*, vol. 3, no. 1, pp. 96–101, 2018.
- [19] W. Liu, N. Mehdipour, and C. Belta, “Recurrent neural network controllers for signal temporal logic specifications subject to safety constraints,” *IEEE Control Systems Letters*, 2021.
- [20] J. P. Vielma and G. L. Nemhauser, “Modeling disjunctive constraints with a logarithmic number of binary variables and constraints,” *Mathematical Programming*, vol. 128, no. 1, pp. 49–72, 2011.
- [21] V. Kurtz, “stlpy: a python library for control from signal temporal logic specifications.” [Online]. Available: <https://github.com/vincekurtz/stlpy>
- [22] S. Boyd, S. P. Boyd, and L. Vandenberghe, *Convex Optimization*. Cambridge university press, 2004.
- [23] R. Tedrake and the Drake Development Team, “Drake: Model-based design and verification for robotics,” 2019. [Online]. Available: <https://drake.mit.edu>
- [24] L. Gurobi Optimization, “Gurobi optimizer reference manual,” 2021. [Online]. Available: <http://www.gurobi.com>
- [25] W. Vega-Brown and N. Roy, “Admissible abstractions for near-optimal task and motion planning,” in *IJCAI*, 2018.